Chemical Physics Letters 501 (2011) 470–474

Contents lists available at ScienceDirect

Chemical Physics Letters

journal homepage: www.elsevier.com/locate/cplett

Controlled synthesis and characterization of single crystalline MnO nanowires and Mn–Si oxide heterostructures by vapor phase deposition

Mohammad Norouzi Banis [a], Yong Zhang [a], Hamid Norouzi Banis [a], Ruying Li [a], Xueliang Sun [a,*], Xinxiang Jiang [b], Darius Nikanpour [b]

[a] Department of Mechanical and Materials Engineering, University of Western Ontario, London, ON, Canada N6A 5B9
[b] Canadian Space Agency, 6767 Route de l'Aeroport, St-Hubert, Quebec, Canada J3Y 8Y9

ARTICLE INFO

Article history:
Received 3 September 2010
In final form 23 November 2010
Available online 26 November 2010

ABSTRACT

High quality mono-phase MnO nanowires were successfully synthesized by vapor phase deposition on a silicon substrate. By involving the silicon into the reaction, MnO nanowires, Mn–Si oxide microwire/nanowall radial heterostructures and silicon oxide nanowires were able to be selectively obtained. The obtained MnO nanowires have a single crystal *fcc* structure with the average diameter of 150 nm and length up to 100 μm. The vapor–solid (VS) mechanism was proposed as the dominant mechanism in growing the MnO nanowires. Controlled synthesis of MnO nanowires provides the possibility of exploring their potential in applications such as catalysts, battery technology and magnetic materials.

1. Introduction

Due to their variable oxidation states, manganese oxides have attracted substantial attention because of their superior magnetic, electrical and chemical properties, which promise great potential in superconductivity [1,2], catalysts [1,3,4], sensors [4], battery [4–8], corrosion resistant [1] and high temperature [1] applications. In recent years, considerable research has been focused on nanostructured manganese oxides. It has been well documented that nanostructured manganese oxides possess unique magnetic [9,10], electronic [11,12] and optical [13] properties, showing quite different behaviors compared to their counterparts in the bulk phase due to their anisotropic features in morphology, size and shape [1,5,8]. For instance, studies on MnO nanoparticles and nanorods have shown that these nanostructures exhibit ferromagnetic behavior while bulk MnO is anti-ferromagnetic [5,9,14]. Seo et al. [15] reported the size dependent magnetic behavior of colloidal Mn_3O_4 and MnO nanoparticles, which can be used for sensor applications. Apart from magnetic properties, it has been reported that MnO nanocrystals have higher oxygen reduction activity compared to bulk MnO in alkaline aqueous solutions [8]. Yang et al. [10] showed that one-dimensional manganese monoxide nanostructures exhibit catalytic function on the oxidation and decomposition of methylene blue dye with H_2O_2. Chen et al. [11] also showed that manganese oxide nanorods have high specific capacitance and a good reversibility, which makes them an excellent candidate as an electrode material for electrochemical capacitors. In addition, properties of the manganese oxide nanostructures can also be readily modified by tailoring their size and structure [8]. More recently, Lahann [16] reported that MnO nanowires could separate water and oil.

In terms of preparation approaches, several methods have been developed to synthesize nanostructured manganese oxides with different morphologies, such as heat treatment of nanostructured precursors of γ-MnOOH [10], thermal decomposition of Mn-Surfactant complexes [5], reflux [18], sol–gel [19] and different types of hydrothermal processes [4,6,17,20–22]. Recently, coral-like Mn_2O_3 nanostructures [12], MnO nanoparticles [23], mixture of MnO and Mn_2O_3 nanowires have been obtained by vapor deposition. However, it still remains a major challenge to synthesize high quality mono-phase MnO nanowires [12,17,23,24] due to the uncontrollable phase transformation of multivalent manganese oxides (MnO_2, Mn_2O_3 and Mn_3O_4).

In the present work, we report a straightforward way of synthesizing high density, single crystalline MnO nanowires with mono-phase using a vapor phase deposition method. In addition, the final product can be tuned between MnO and SiO_2 nanowires as well as their heterostructures by controlling experimental parameters. The influence of experimental parameters on the final product was systematically investigated and the growth mechanism of the products was proposed.

2. Experimental procedure

Manganese oxide nanowires on a silicon substrate were synthesized by a simple vapor phase deposition method. In this method, metallic manganese powder (99%, Aldrich) was used as the source material. Before the growth procedure, a silicon wafer was coated

* Corresponding author.
E-mail address: xsun@eng.uwo.ca (X. Sun).

0009-2614/$ - see front matter © 2010 Elsevier B.V. All rights reserved.
doi:10.1016/j.cplett.2010.11.078

with a 5 nm thin gold layer as catalyst using an Emitech K550X sputter coater. The manganese source was placed in an alumina boat and the silicon substrate (Si) was placed over the powder covering the source. The distance between the powder and the substrate was carefully controlled. The boat was placed at the center of a quartz tube and transferred into a horizontal high temperature resistance furnace. The system was heated to 900–1000 °C at controlled heating rates (5–50 °C min^{-1}) for 2 h. During the process a constant flow of high purity argon (200 sccm) was maintained. Various parameters such as the temperature of the system, heating rate and source/substrate distance were varied to control the morphology and structure of the products. After the furnace was cooled down to room temperature, the final products were collected from the substrate and the Mn powder.

The morphology, structure and composition of the resultant products were characterized by Hitachi S-4500 field-emission scanning electron microscope (SEM) operated at 5.0 kV and energy dispersive X-ray spectrometer (EDX), Rigaku–Miniflex X-ray diffractometer, using CuKα ($\lambda = 0.154$ nm) radiation operated at 30 kV and 15 mA, Philips CM10 transmission electron microscope (TEM) and selected area electron diffraction(SAED) operated at 80 kV, a Jeol 2010 field emission gun high resolution electron microscope (HRTEM) operated at 200 kV and Kratos Axis Ultra Al(alpha) X-ray photoelectron spectrometer (XPS) operated at 14 kV.

3. Results and discussion

Manganese oxide nanowires were synthesized on a silicon substrate after optimization of various growth parameters. The general morphology of the products was initially observed by SEM. Figure 1a shows a typical SEM image of the product. It reveals that the product consists of dense nanowires with sharp tips that cover the silicon substrate uniformly. The length of the resultant nanowires is up to 100 μm. Furthermore SEM observations of the cross section of nanowires deposited on the silicon substrate (Figure 1b) indicate the formation of layer between the substrate and nanowires with a thickness of around 100 nm. EDX results from this layer reveal that this layer is mainly composed of manganese, oxygen and silicon. The EDX spectrum of the nanowires, as shown in Figure 1c, indicates that the nanowires are mainly composed of manganese and oxygen. The weak silicon peak in the spectrum comes from the substrate and the intermediate layer. Figure 1d displays the XRD pattern taken from the products on silicon substrate. The main diffraction peaks at this spectrum are assigned to the (1 1 1), (2 0 0), (2 2 0), (3 1 1) and (2 2 2) crystal planes of MnO (PDF No. 07-0230), respectively, indicating that the nanostructures have well-crystallized face centered cubic (*fcc*) MnO crystal structure. In addition to these peaks, several weaker peaks can be identified in the XRD pattern which roughly can be assigned to compounds of manganese, silicon and oxygen such as Mn_2SiO_4 (PDF No. 35-0748).

TEM observations indicate that diameter of the nanowires ranges from 70–300 nm with a mean value of 150 nm. Figure 2a shows a typical TEM image of a single nanowire with a diameter of around 170 nm. The selected area electron diffraction (SAED) pattern (Figure 2b) taken from this nanowire reveals the single crystalline nature of the nanowire and the reflections can be indexed as the (1 1 1), (2 0 0) and (1 $\bar{1}$ $\bar{1}$) crystal planes of the *fcc* MnO phase, which is consistent the XRD results. HRTEM analysis (Figure 2c) of manganese monoxide nanowires shows that the nanowire possesses a relatively smooth surface. The lattice fringes in Figure 2c clearly confirm the high quality crystallinity of the nanowire. The inter-planar spaces measured as 0.25, 0.25 and

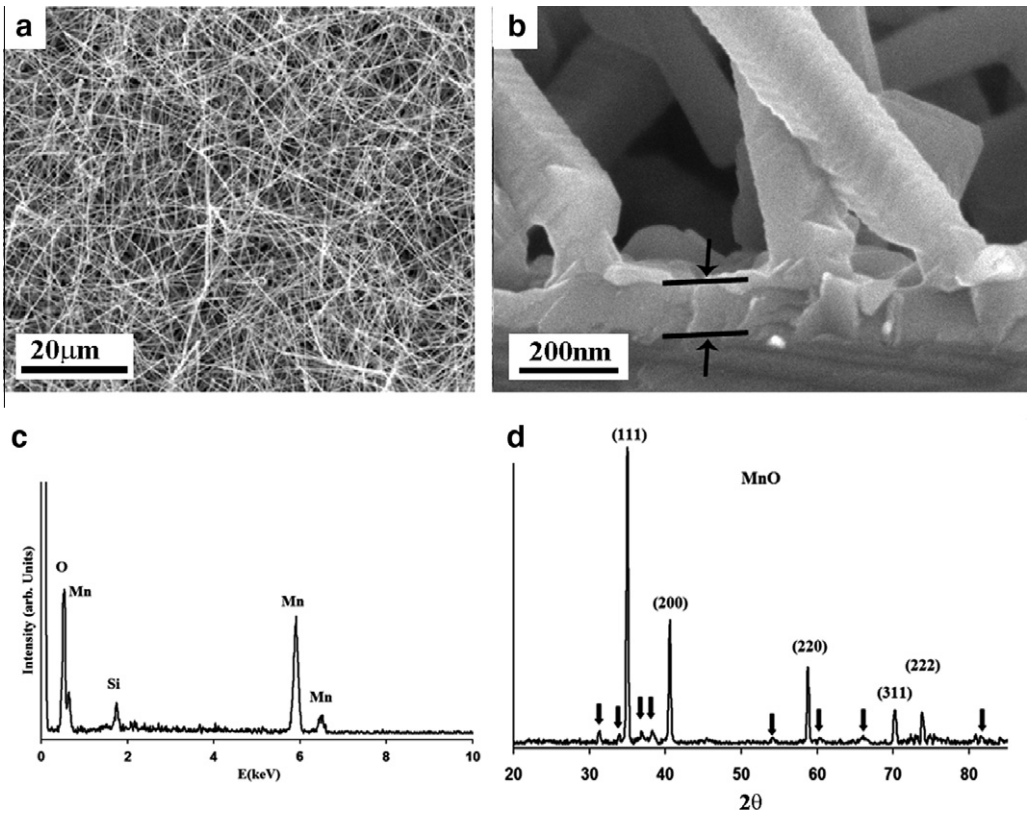

Figure 1. (a) SEM images of manganese oxide nanowires synthesized on a silicon substrate, showing uniform coverage of manganese oxide nanowires. (b) EDX spectrum of manganese oxide nanowires. (c) XRD pattern of these nanowires on a silicon substrate.

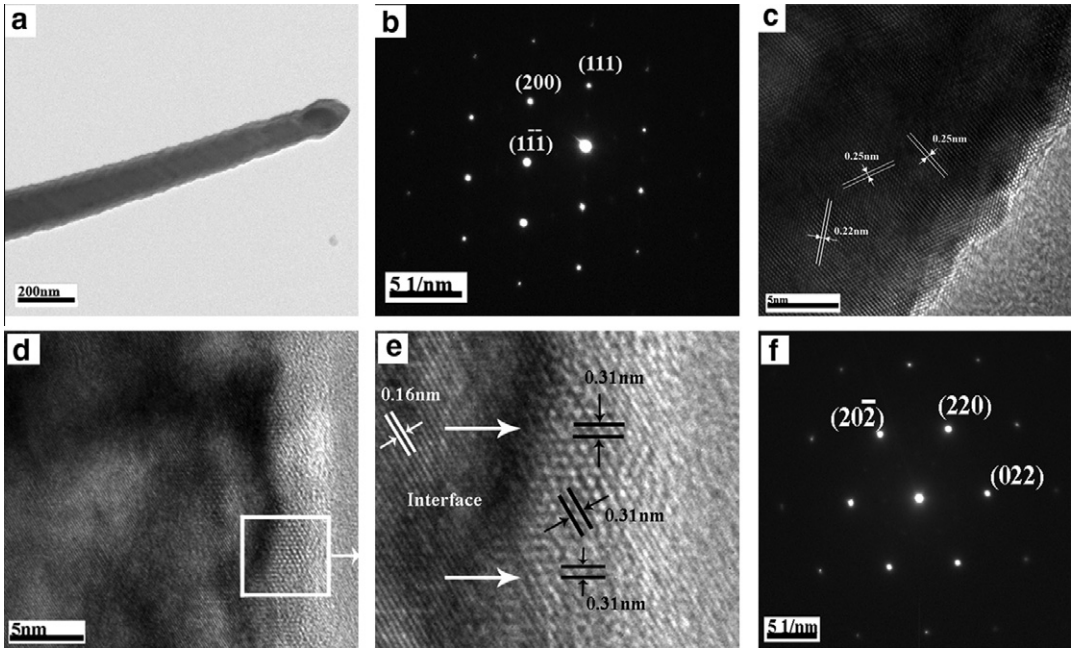

Figure 2. (a) TEM image of a MnO nanowire with a diameter of about 170 nm. (b) SAED pattern of the nanowires corresponding to *fcc*-MnO phase. (c) HRTEM image of single manganese oxide nanowires. (d) HRTEM image of MnO core–shell nanostructure. (e) HRTEM image of crystalline shell. (f) SAED pattern of the core shell nanostructure.

0.22 nm corresponding respectively to the (1 1 1), (1 $\bar{1}$ $\bar{1}$) and (2 0 0) planes of MnO crystal structure. Further HRTEM analysis of manganese monoxide nanowires reveals some regions of the nanowires exhibit core/shell structures (Figure 2d). Core shell formation of MnO nanostructures has been reported by other researchers synthesizing manganese monoxide nanoparticles [5]. This has been related to the formation of more stable manganese oxides on the outer layers of the nanostructures. In this study the shell layer has a distinct interface with the inner part shown in Figure 2e. The three inter-planar spacing of these layers measured as 0.31 nm suggest a cubic structure similar to the crystal structure of MnO nanowires. The SAED pattern of these nanowires shown in Figure 2f can be indexed as the crystal planes of the *fcc* MnO phase similar to previous pattern. However in this pattern there are very week reflections which can be related to the crystal layer covering the nanowires. This shell layer can be related to the partial oxidation of MnO nanowires in room temperature forming a more stable manganese oxide on the nanowires.

During our experimental process, it has been found that the morphology of the structures is very sensitive to the growth parameters, such as synthesis source/substrate distance, and heating rate of the reaction system. In order to control the nanostructures and to understand the growth mechanism of the MnO nanowires, the effects of the growth parameters on the nanowires composition and structure were systematically studied.

3.1. Effect of source/substrate distance

The source/substrate distance was found to be a significant factor affecting not only the morphology but also composition and phase structure of the nanostructure. When the distance of source/substrate is less than 2 mm in the chamber, manganese oxide nanowires were obtained. Upon increasing the source/substrate distance to more than 6 mm, the substrate was covered with high density thin and tangled nanowires with the morphology completely different from the manganese oxide nanowires mentioned above, as shown in Figure 3a. XPS results in Figure 3b indicate that the nanowires consist of silicon and oxygen with a stoichiometry ratio of 1 to 2 (SiO_2). TEM and SEM observations reveal that SiO_2 nanowires have a narrow diameter range of about 70 nm. The electron diffraction pattern shown in inset of Figure 4a indicates the amorphous nature of these nanowires. When the source/substrate distance was kept at 4 mm, the products were composed of a mixture of manganese oxide nanowires and silicon oxide nanowires. The detailed growth mechanisms will be discussed in section 3.3.

3.2. Effect of heating rate

In our previous studies of growing various metal oxide nanowires such as SnO_2, and $W_{19}O_{48}$ nanowires [25,26] by the chemical vapor deposition method, we found that the formation of these nanowires is not sensitive to heating rate. In the current work, however, it has been observed that the final composition and structure of the product has a strong dependence on the heating rates of the reaction system. We found that a low heating rate favored the deposition of manganese oxide nanowires (5 °C min^{-1} in this case), while keeping other optimized conditions (930 °C, 2 mm source/substrate distance) (Figure 1). The morphology of deposited structures changed dramatically by increasing the heating rate of the process while keeping the other conditions unchanged. Figure 4a shows a low magnification SEM image of microstructures covering the substrate uniformly with high density deposited at a heating rate of 50 °C min^{-1}. Higher magnification SEM image in Figure 4b reveals that these structures are composed of microwires covered by epitaxial nanowalls. It can be seen that the microwires are composed of network of nanowires surrounding a shell microwire. To determine the composition of these composite structures, they were analyzed using EDX mapping. The EDX mapping of a single composite structure indicates the microwires are mainly composed of manganese, oxygen and silicon. On the nanowalls, however, mostly silicon and oxygen are detected, along with very small trace of manganese, indicating a heterostructure of Si–Mn oxide product. Our experimental results have shown that increasing the heating rate (5 to 50 °C min^{-1}) favors the growth of the heterostructure and restrains the deposition of manganese oxide nanowires. Further

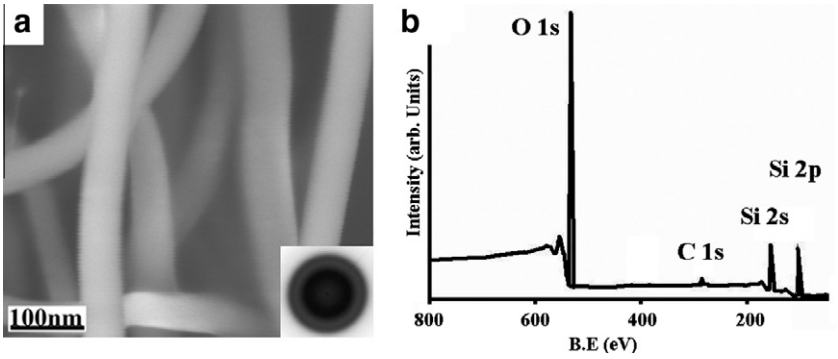

Figure 3. (a) SEM images of silicon oxide nanowires with diameters below 100 nm synthesized by increasing the distance between manganese powder and silicon substrate to more than 5 mm. (b) XPS results of these nanowires showing 1:2 atomic ratio of Si:O, indicating that these nanowires are mainly SiO_2 nanowires.

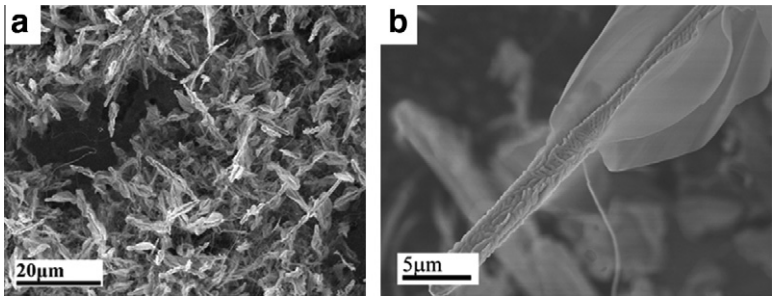

Figure 4. SEM images of structures synthesized by increasing the heating rate of the experiment to 50 °C min^{-1}. (a) low magnification SEM image showing high-density microstructures, (b) higher magnification SEM images shows that these structures are composed of micro-wires as core with sheet-like structures covering these wires.

experiments on control and characterization of these structures are being carried out in our group.

The effects of growth parameters of MnO nanowires on the morphology of nanostructures deposited on silicon substrate are summarized in Table 1. Based on these results a growth mechanism has been proposed in the following section.

3.3. Growth mechanism

Vapor–liquid–solid (VLS) process has previously been reported for the growth of MnO nanowires [23,24]. In the present study, similar to previous studies a thin layer of gold was sputtered on the substrate to act as the gold catalyst but based on TEM and SEM observations no obvious gold particles were detected on the tip of MnO nanowires. Furthermore, as mentioned above SEM and EDX studies of the cross section of the interface between the nanowires and silicon substrate has shown a intermediate layer which is composed of manganese, oxygen and silicon (Figure 1b and c). XRD pattern (Figure 1d) revealed the presence of Mn_2SiO_4 layer on the substrates. Experimental results show that the formation of this layer is essential for the formation of high density thin MnO nanowires. However the formation of this layer is dependant on the presence of gold layer and high Mn partial pressure. Therefore, we propose a vapor solid mechanism (VS) here to interpret the growth of manganese oxide nanowires. Figure 5 shows a schematic diagram of manganese oxide nanostructures growth mechanism. Based on this mechanism the growth of MnO nano and microstructures directly from Mn powder and thin films as byproducts of these experiments can be explained.

According to this mechanism, Au–Si alloy droplets can be formed during the heating process due to the very low eutectic point (363 °C, [27]) of Au–Si alloy. The liquid surfaces have a large accommodation coefficient and are therefore preferred deposition sites for the incoming vapor [28]. In this case, both manganese and

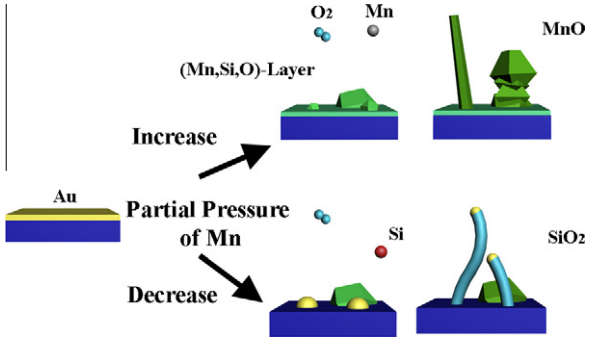

Figure 5. Schematic diagram of manganese oxide nanostructure growth mechanism.

silicon atoms are absorbed by the liquid droplets, in which manganese source is from the evaporated manganese powder and silicon source is from the silicon substrate. When the distance between the Mn powder and silicon substrate was very close (2 mm), concentrated manganese species were easily absorbed into the semi-liquid alloy droplets increasing their size and eventually forming a thin layer composed of the three elements. This layer similar, to oxidized manganese source powder provides a suitable surface for the deposition of MnO as nanowires by absorption and reaction of residual oxygen in the system with Mn species.

As discussed above, the effect of various parameters on the morphology, composition and structure of the product is supposed to be related to species and pressure of the formed gaseous atoms in the reaction chamber. For the source/substrate distance factor, the distance directly influenced the amount of manganese vapor reaching the substrate. According to previous reports, it is possible to synthesize silicon oxide nanowires directly from the silicon substrate using gold as a catalyst governed by solid–liquid–solid (SLS)

Table 1
Summary of the effect of growth parameters on the morphology of nanostructures deposited on silicon substrate.

Temperature (°C)			Source/substrate Dist. (mm)			Heating rate (°C min^{-1})		Deposited nanostructure
900	930	960	2	2–6	6	5	50	
	*		*			*		MnO nanowire
*			*			*		MnO nanoparticle
		*	*			*		Non-uniform diameter MnO nanowire
	*			*		*		MnO nanowire & SiO*x* nanowire mixture
	*				*	*		SiO2 nanowire
	*		*				*	MnO-SiO*x* Composite structure

[29,30] mechanism in similar experimental conditions. Under the conditions in the present study, there is a competition between the growth of manganese oxide nanowires and silicon oxide nanowires depending on the degree of supersaturation of manganese and silicon species within the liquid alloy droplets. At short distances, the substrate is exposed to a concentrated manganese vapor enabling higher degree of supersaturation of manganese species than that of silicon within the liquid droplets, in which the silicon atoms diffusion is restricted. Therefore, manganese oxide nanowires are preferentially formed. At larger distances, when the decrease of local manganese concentration slows down the growth of manganese oxide nanowires, the growth of silicon oxide nanowires is enhanced. Therefore, the density of silicon oxide nanowires increases with increasing the source/substrate distance, and finally only silicon oxide nanowires are synthesized at long distances.

In contrast to the growth of silicon oxide nanowires, which is independent of the heating rate, the achievement of manganese oxide nanowires is determined to a great extent by the control of the heating rate. As is known, oxygen partial pressure is a function of temperature and increases with increasing temperature [31]. Depending on the evaporation and oxidation dynamics of the manganese in the system, a higher heating rate might give a quick increase of the oxygen partial pressure in the chamber, which possibly led to high oxidizing rate of the manganese powder and decreased the vapor pressure of manganese. Hence, a high heating rate would increase the possibility of growth of silicon oxide structures from the substrate and would also explain the low density and thick diameter of the manganese oxide structures. Therefore, the growth parameters have to be carefully controlled to obtain manganese monoxide nanowires as the sole phase structure.

4. Conclusions

In summary, high quality and single crystalline MnO nanowires were successfully synthesized using a simple vapor phase deposition method on a silicon substrate with a thin layer of gold. SEM observations showed dense and uniform growth of the nanowires with the length up to 100 μm. HRTEM images and SAED patterns provided evidence of the single crystalline, face centered cubic nature of the MnO nanowires. By tuning the growth parameters, MnO nanowires, Mn–Si oxide microwire/nanowall heterostructures or SiO_2 nanowires can be selectively obtained depending on the competitive growth rates of manganese oxide or silicon oxide. The controlled synthesis of MnO nanowires and their heterostructures are expected to find applications in nanodevice technologies. In addition the obtained MnO nanowires can provide suitable precursors to synthesize other types of manganese oxide nanostructures such as MnO_2, Mn_2O_3 and Mn_3O_4.

Acknowledgments

This research was supported by the Natural Sciences and Engineering Research Council of Canada (NSERC), the Canadian Space Agency, the NSERC Canada Research Chair (CRC) Program the Canada Foundation for Innovation (CFI), the Ontario Research Fund (ORF), the Ontario Early Researcher Award (ERA) and The University of Western Ontario. We are in debt to David Tweddell for his kind help and fruitful discussions.

References

[1] S.K. Nayak, P. Jena, J. Am. Chem. Soc. 121 (1999) 644.
[2] C.N.R. Rao, B. Raveau, Transition metal oxides, VCH Publishers Inc., New York, 1995.
[3] N.A.M. Barakat, K.D. Woo, S.G. Ansari, J.A. Ko, M.A. Kanjwal, H.Y. Kim, Appl. Phys. A 95 (2009) 769.
[4] D. Yan et al., Chem. Phys. Lett. 440 (2007) 134.
[5] J. Park et al., J. Phys. Chem. B 108 (2004) 13594.
[6] Y. Chen, Y. Zhang, Q.Z. Yao, G.T. Zhou, S. Fu, H. Fan, J. Solid State Chem. 180 (2007) 1218.
[7] G.H. Du, Z.Y. Yuan, G.V. Tendeloo, Appl. Phys. Lett. 86 (2005) 063113.
[8] S. Shanmugam, A. Gedanken, J. Phys. Chem. B 110 (2006) 24486.
[9] M. Ghosh, K. Biswas, A. Sundaresan, C.N.R. Rao, J. Mater. Chem. 16 (2006) 106.
[10] Z. Yang, Y. Zhang, W. Zhang, X. Wang, Y. Qian, X. Wen, S. Yang, J. Solid State Chem. 179 (2006) 679.
[11] H. Chen et al., J. Mater. Chem. 17 (2007) 855.
[12] K. Ramesh, L. Chen, F. Chen, Z. Zhong, J. Chin, H. Mook, Y.F. Han, Catal. Commun. 8 (2007) 1421.
[13] G. An, P. Yu, M. Xiao, Z. Liu, Z. Miao, K. Ding, L. Mao, Nanotechnology 19 (2005) 275709.
[14] G.H. Lee, S.H. Huh, J.W. Jeong, B.J. Choi, S.H. Kim, C.H. Ri, J. Am. Chem. Soc. 124 (2002) 12094.
[15] W.S. Seo, H.H. Jo, K. Lee, B. Kim, S.J.J. Oh, J.T. Park, Angew. Chem. Int. Edit. 43 (2004) 1115.
[16] J. Lahann, Nat. Nanotechnol. 3 (2008) 320.
[17] X. Wang, Y. Li, Chem. Eur. J. 9 (2003) 300.
[18] N. Kijima, H. Yasuda, T. Sato, Y. Yoshimura, J. Solid State Chem. 159 (2001) 94.
[19] C. Shao, H. Guan, Y. Liu, X. Li, X. Yang, J. Solid State Chem. 177 (2004) 2628.
[20] V. Subramanian, H. Zhu, R. Vajtai, P.M. Ajayan, B. Wei, J. Phys. Chem. B 109 (2005) 20207.
[21] L.X. Yang, Y.j. Zhu, W.W. Wang, H. Tong, M.L. Ruan, J. Phys. Chem. B 110 (2006) 6609.
[22] L.X. Yang, Y.J. Zhu, H. Tong, W.W. Wang, G.F. Cheng, J. Solid State Chem. 179 (2006) 1225.
[23] C.W. Na, D.S. Han, D.S. Kim, J. Park, Y.T. Jeon, G. Lee, M.H. Jung, Appl. Phys. Lett. 87 (2005) 142504.
[24] Y.Q. Chang, D.P. Yu, Y. Long, J. Xu, X.H. Luo, R. Ye, J. Cryst. Growth 279 (2005) 88.
[25] R. Li, X.C. Sun, Y. Zhou, M. Cai, X. Sun, J. Phys. Chem. C 111 (2007) 9130.
[26] M.S. Saha, R. Li, M. Cai, X. Sun, Electrochem. Solid-State Lett. 10 (2007) B130.
[27] H. Okamoto, Desk hand book: phase diagram of binary alloys, ASM International, USA, 2000.
[28] C.N.R. Rao, F.L. Deepak, G. Gundiah, A. Govindaraj, Prog. Solid State Chem. 31 (2003) 5.
[29] H.K. Park, B. Yang, S.W. Kim, G.H. Kim, D.H. Youn, S.H. Kim, S.L. Maeng, Physica E 37 (2007) 158.
[30] Y.J. Xing, Z.H. Xi, D.P. Yu, Q.L. Hang, H.F. Yan, S.q. Feng, Z.Q. Xue, Chin. Phys. Lett. 19 (2002) 240.
[31] C.Y. Wang, L.H. Chan, D.Q. Xiao, T.C. Lin, H.C. Shih, J. Vac. Sci. Technol., B 24 (2006) 613.